Available online at www.sciencedirect.com
ScienceDirect
Bioorganic & Medicinal Chemistry Letters
Bioorganic & Medicinal Chemistry Letters 17 (2007) 4812–4818

Novel inhibitor for fibroblast growth factor receptor tyrosine kinase

Naparat Kammasud,[a] Chantana Boonyarat,[b] Satoshi Tsunoda,[c] Hiroaki Sakurai,[c] Ikuo Saiki,[c] David S. Grierson[d] and Opa Vajragupta[a,*]

[a]*Department of Pharmaceutical Chemistry, Faculty of Pharmacy, Mahidol University, 447 Sri-Ayudhya Road, Bangkok 10400, Thailand*
[b]*Faculty of Pharmaceutical Sciences, Khon Kaen University, Khon Kaen 40002, Thailand*
[c]*Division of Pathogenic Biochemistry, Department of Bioscience, Institute of Natural Medicine, University of Toyama, Japan*
[d]*UMR 176 CNRS, Institut Curie, Section Recherche, Centre Universitaire, Bat.110-112, 91405 Orsay cedex, France*

Received 16 March 2007; revised 8 June 2007; accepted 18 June 2007
Available online 26 June 2007

Abstract—NP603, the 6-dimethoxy phenyl indolin-2-one, was designed as FGF receptor 1 inhibitor by computational study. NP603 was synthesized and found to be more active against endothelial proliferation of HUVEC after the rhFGF-2 stimulation than SU6668 with minimum effective dose of 0.4 μM but with similar potency as SU16g. NP603 inhibited the tyrosine phosphorylation in FGF receptor and the activation of extracellular signal-regulated kinase and c-Jun-N-terminal-kinase after the rhFGF-2 stimulation. The increase in activity of NP603 supports the role of Lys514 movement in ligand–receptor binding in modeling study as the movement accommodates the hydrophobic interaction at the receptor pocket leading to the enhancement of binding capacity.

Receptor tyrosine kinases (RTKs) have been shown to be important mediators of signal transduction in cells.[1–5] These transmembrane molecules characteristically consist of an extracellular ligand-binding domain connected through a segment in the plasma membrane to an intracellular tyrosine kinase domain. Binding of the ligand to the receptor results in receptor dimerization and stimulation of the receptor-associated tyrosine kinase activity, which leads to phosphorylation of tyrosine residues on both the receptor and other intracellular molecules. These changes in tyrosine phosphorylation initiate a signaling cascade leading to a variety of cellular responses, one of which is angiogenesis.[6,7] Growth factors, including the vascular endothelial growth factors (VEGF), the fibroblast growth factors (FGF), and the platelet-derived growth factors (PDGF) and their associated receptor tyrosine kinases, are major regulators of angiogenesis.

RTKs are important therapeutic targets for cancer drug discovery and development. Amongst the many inhibitors undergoing development, 3-substituted indolin-2-ones were found to exhibit high potency and selectivity against PDGF and VEGF (Flk-1) RTKs. SU5402 and SU5416 have been shown to be specific inhibitors of the kinase activity of the fibroblast growth factor receptor (FGFR) and vascular endothelial growth factor receptor (VEGFR), respectively, whereas SU6668 showed inhibitory activity against FGFR, VEGFR, and PDGFR.[8,9] The pyrido[2,3-*d*]pyrimidine PD173074, a potential drug candidate, was similarly found to be highly selective for the FGFR1. This molecule is a nanomolar inhibitor of FGFR1 and is also a submicromolar inhibitor of VEGFR2. Structure–activity relationship (SAR) data for compounds in the pyrido[2,3-*d*]pyrimidine series indicate that binding affinity and selectivity for FGFR1 is attained through modification of the phenyl group attached to the 6-position of the pyrido[2,3-*d*]pyrimidine scaffold. In general, derivatization at the 3- and 5-positions of the phenyl ring increases selectivity for FGFR1, especially when the attached group is larger than a methyl. The SAR data are in good agreement with the surface observed in the structure for PD173074 bound in the FGFR1 kinase domain (PDB accession code 2FGI).[10]

Keywords: FGFR1; FGFR1 inhibitor; SU6668; Phenyl indolin-2-one; Docking; Binding mode; Antiproliferation; Antiangiogenesis.
* Corresponding author. Tel.: +66 2 6448677; fax: +66 2 6448695; e-mail: pyovj@mahidol.ac.th

0960-894X/$ - see front matter © 2007 Elsevier Ltd. All rights reserved.
doi:10.1016/j.bmcl.2007.06.058

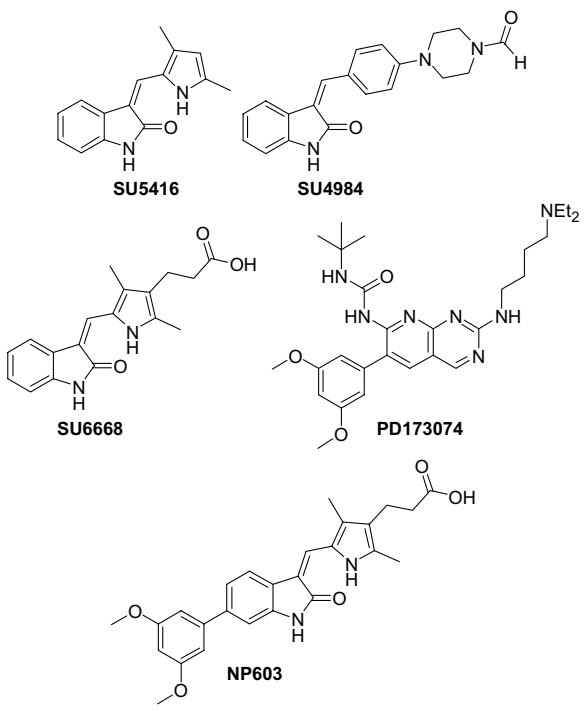

Through superposition of the SU5402-FGFR1 structure (1FGI) with 2FGI it was determined that the conserved Lys514 undergoes significant movement upon PD173074 binding. The side chain of Lys514 adopts an alternative conformation which allows the dimethoxy phenyl substituent of PD173074 access to the back of the ATP-binding cleft.

On comparison of indolinones, such as SU4984, SU5402, and SU6668 to PD173074, certain structural similarity may be noticed, and in particular, a NH (hydrogen donor) and an aromatic group. Figure 1 provides the schematic drawing of the binding mode between FGFR1 and the inhibitors based on these different scaffolds.

SAR studies on the indolin-2-one series suggested that modifications at the C-6 position would lead to compounds with different kinase inhibition profiles for VEGFR2 (Flk-1) and FGFR1. However, the structural information from the protein binding study of PD173074 indicated that the contribution of the dimethoxy phenyl group to tight binding in 1FGFR is important. Therefore, structural modification of the indolin-2-ones to include this dimethoxy phenyl motif at position 6 should, in principle, lead to a potent 1FGFR inhibitor. This reasoning suggested that the novel C-6 substituted oxindole analog (NP603) may be an interesting probe in modeling studies to ascertain the role of Lys514 movement in ligand–receptor binding.

In this study, the proposed compound NP603 was flexibly docked to the model of the constructed FGF1 receptor template. The goal was to study the effects of the added substituent at 6-position on the structure and the orientation of the ligand–receptor complex. In addition to docking studies, NP603 was synthesized and evaluated for its activity.

The crystal structure of FGFR1 bound to the inhibitor PD173074 (Protein Data Bank code: 2FGI[10]) was selected for the construction of the docking template. In order to prepare the target protein as a template, the ligand and crystallographic water were removed. Hydrogens and Kollman unified charges were added by using AutoDockTools (ADT).[11] Cubic affinity grid maps for each atom type in the ligand set (plus an electrostatics map) centered on the cavity with dimensions of $60 \times 60 \times 60$ Å and 0.375 Å spacing between grid points were computed using AutoGrid 3.0. The constructed FGFR1 template was validated by redocking with the native ligand, PD173074, AutoDock 3.0.5 was employed to perform the docking calculation. All ligands were created and initially optimized with SYBYL7.0. All protons were added, charges were assigned using the Gasteiger–Hückel method, and ligand energies were minimized using the TRIPOS force field. During final preparations Kollman charges were added, nonpolar hydrogens and lone pairs were merged, aromatic carbons identified, and lastly, the rigid root and rotatable bonds were defined. The 3D configuration of PD173074, obtained from docking with the constructed FGFR1 template, was compared with the crystallographic pose. PD173074 docked in the binding pocket

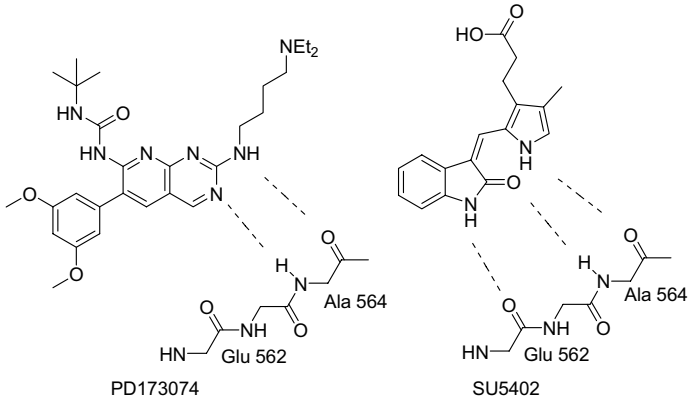

Figure 1. The binding modes of the FGFR1 kinase and the inhibitors: SU5402 and PD173047.

in the conformation found in the crystal structure. The result showed the same configuration with RMSD of 1.6 Å when compared with the crystal structure of PD 173074 in complex with the tyrosine kinase domain of FGFR1.

In order to study the binding mode, SU6668, NP603, and related analogs (unsubstituted phenyl and methoxy substituted phenyl at position 6, SU16f and SU16g) were docked with the validated FGFR1 template. A computational docking study using Autodock supports that the binding cleft for the ATP domain of FGFR1 is the target area for the inhibitors. The binding mode of NP603, which was designed by substitution of dimethoxy phenyl group at the 6-position of indolin-2-one to enhance the binding capacity via the hydrophobic interaction at the receptor pocket, is shown in Figure 2. The docking studies confirmed that the added substituent locates in the pocket and contributes to the hydrophobic type interaction as expected. The docking energy of NP603 is −13.3 kcal/mol, the lowest amongst the inhibitors studied (Table 1).

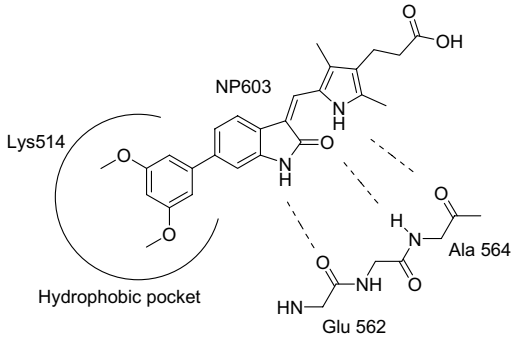

Figure 2. The binding modes of the FGFR1 kinase and NP603.

Figure 3 shows the superposition of the oriented conformations of the inhibitors (SU6668 and NP603) docked to the FGFR template, with the conformation of PD173074 from X-ray crystal structure. It was observed that the docked conformations of the inhibitors showed very similar orientations of binding on FGFR1.

The docked orientation of NP603 showed that the substituted moiety at position 6 located near to the active binding site of the substrate. This molecule makes three hydrogen bonds to the protein backbone of

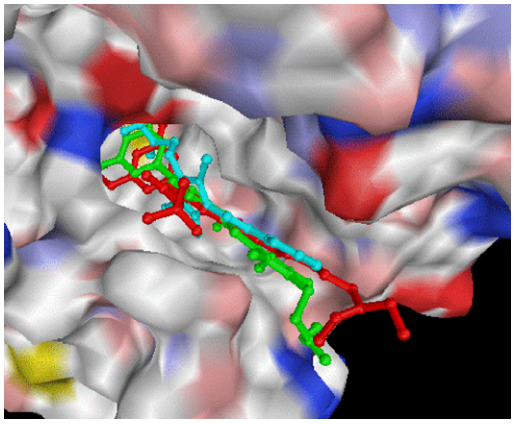

Figure 3. Superposition of crystallographic PD173074 binding position (red stick model) and docked orientations of inhibitors: NP603 (green) and SU6668 (blue) bound to FGFR1 template.

Table 1. Effect on the proliferation of HUVEC after the rhFGF-2 stimulation

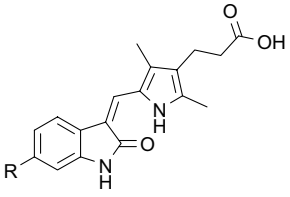

	R	Binding energy (kcal/mol)	Docking energy (kcal/mol)	Concentration (μM)	
				IC_{50}	Min effective
SU6668	H	−8.49	−10.2	>50.0	10
SU16f[9]		−11.3	−13.2	>50.0	10
SU16g[9]	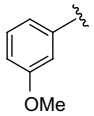	−11.0	−13.0	17.9	0.4
NP603	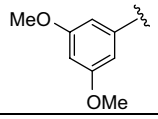	−11.5	−13.3	18.2	0.4

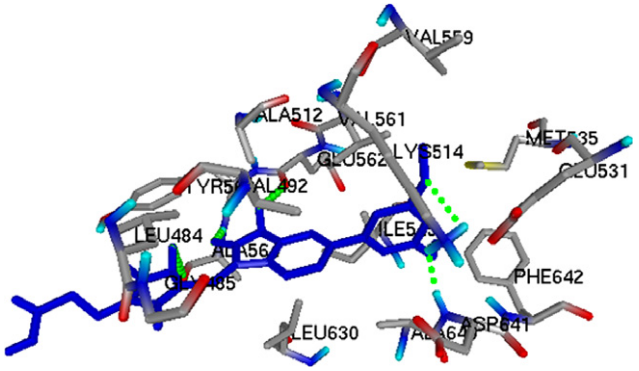

Figure 4. Hydrogen bonds (green spheres) between NP603 (blue) and FGFR1 template.

FGFR1: between N-1 of the oxindole and the carbonyl oxygen of Glu562, between carbonyl oxygen of the oxindole and the amide nitrogen of Ala564, and between N-1 of the pyrrole and the carbonyl oxygen of Ala564 (Fig. 4). This same two residues Glu562 and Ala564, located in the hinge region of FGFR1, are involved in hydrogen bonds to N-1 and N-6 in the adenine ring of ATP. The hydrophobic residues, Val559 and Val561, appear to be involved in the interaction with the 3,5-dimethoxy group of NP603. In addition to three hydrogen bonds involving the oxindole scaffold, the oxygen atoms of the two methoxy groups in NP603 contribute two hydrogen bonds. One is made between the methoxy group of NP603 and the amide nitrogen of Asp641, and the other between the other methoxy group of NP603 and the amide nitrogen of Lys514. van der Waals contacts are made between the dimethoxy phenyl group and the side chains of Lys514, Glu531, Met535, Ile545, Val559, Val561, Ala640, and Phe642 (Fig. 4).

According to the derived docking model of SU6668 (the indolinone scaffold without substitution on position 6) two hydrogen bond interactions were formed between the N and O of the oxindole with Ala564. We found that the docked conformation of SU6668 was flipped when compared with the crystal structure of SU5402 in 1FGI (Fig. 1). This was because the FGFR1 template in this study was developed from the crystal structure of PD173074 with the alternative conformation involving Lys514 movement to accommodate hydrophobic interaction. For PD173074 and NP603, the docking results showed that the dimethoxy phenyl substitution at position 6 fitted the hydrophobic pocket creating van der Waals interactions between the 6-substituted aromatic ring and Val559 and Val561. According to the docked conformation of NP603, a total of seven hydrogen bonding interactions were found.

As NP603 demonstrated good binding with FGFR1 in silico, NP603 and the related compounds SU6668, SU16f, and SU16g were synthesized and evaluated for their activity in vitro. The synthesis of NP603[12] was accomplished by the synthetic routes A and B. The 6-substituted indolin-2-one [**4**] was prepared in four steps (1.1 g, 25%), involving: reaction of 3,5-dimethoxyphenyl boronic acid (6.9 g, 56.5 mmol) and 5-bromo-2-fluoronitrobenzene (0.2 ml, 14.1 mmol) under Suzuki conditions, to give 5-aryl-2-fluoronitrobenzene [**1**] (2.51 g, 75%), displacement of the o-fluoro substituent by dimethyl malonate (1.38 g, 34.5 mmol) followed by hydrolytic decarboxylation using 6 N aqueous hydrochloric acid and cyclization (Scheme 1). NP603 (80 mg, 20%) was obtained by condensation of 6-substituted indolin-2-one [**4**] (15 mg, 1.1 mmol) with pyrrole aldehyde [**5**] (22 mg, 1.1 mol) (Scheme 2). The structure of synthesized compound was characterized by their melting points, FTIR, ^{1}H NMR, ^{13}C NMR, MS, and elemental analyses of C, H, and N. Spectral data (FTIR, NMR, and MS) were compatible with the assigned structures in all cases.

The in vitro kinase assay of NP603 was performed. The effect on the activity of the human FGFR1 kinase expressed in insect cells was quantified by measuring the phosphorylation of the substrate biotinyl-βAβA-βAAAEEEYFFLFAKKK and the HTRF detection method.[13] The IC_{50} against FGFR1 was found to be 0.4 μM, three times less than that of SU16g (IC_{50} 1.2 μM). FGF-2 is known to be one of the potent mitogens of vascular endothelial cells and to play an important role in the tumor-induced angiogenesis. Therefore,

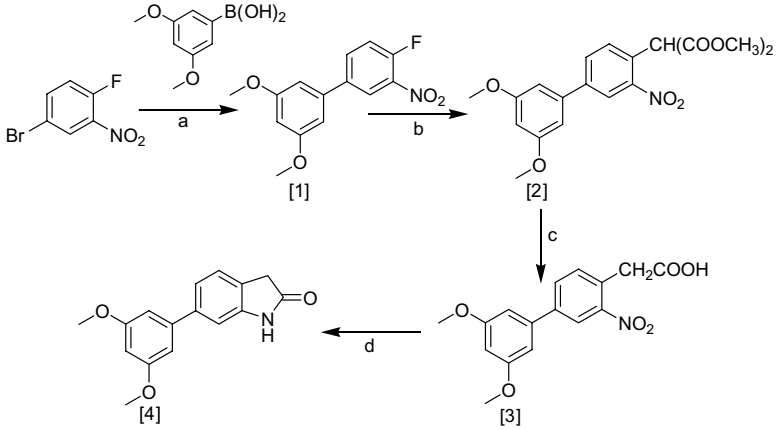

Scheme 1. Synthesis of 6-substituted indolinone. Reagents and conditions: (a) $(Ph_3P)_4Pd$, $NaHCO_3$, toluene–ethanol, reflux, 2 h; (b) $CH_2(COOCH_3)_2$, NaH, THF, 100 °C, 2 h; (c) 6 N HCl_{aq}, overnight; (d) Pd/C, H_2, HOAc, rt, 2 h.

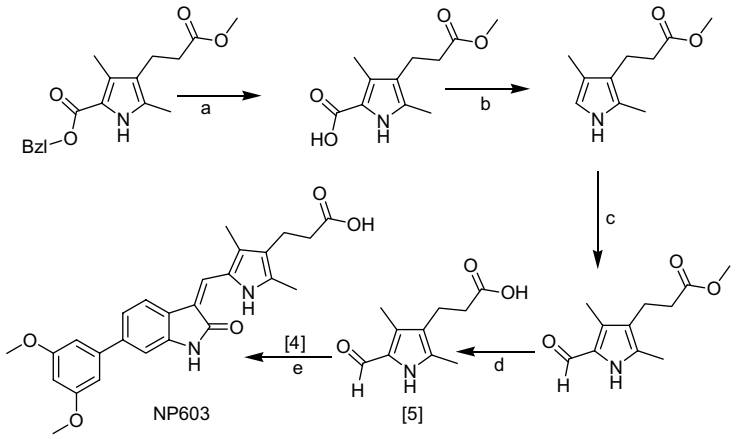

Scheme 2. Synthesis of NP603. Reagents and conditions: (a) Pd/C, H2, ethanol, rt, 2 h; (b) TFA, reflux, 1 h; (c) TFA, trimethyl orthoformate, reflux, 1 h; (d) $NaOH_{aq}$, reflux, 2 h; (e) 6-substituted indolin-2-one, piperidine, ethanol, reflux, 3 h, then 2 N HCl_{aq}.

we determined the effect of NP603 and related compounds on the proliferation of human umbilical vein endothelial cells (HUVEC) after the recombinant human FGF-2 (rhFGF-2) treatment. All the tested compounds inhibited the rhFGF-2-induced cellular proliferation of HUVEC. NP603 has the highest inhibitory effect among the compounds. The SU16g[9] and NP603 bearing methoxyl group on phenyl ring were highly active against endothelial proliferation, as compared with SU6668 and the unsubstituted SU16f[9]. The minimum effective concentrations of NP603 and SU16g are 0.4 μM. The degree of inhibition correlates with the binding energy obtained from the docking study (Table 1). The minimum cytotoxic concentration of NP603 in the absence of rhFGF-2 was found to be 50 μM, which is one hundred times greater than the minimum effective dose.

The effect on the intracellular signaling in HUVEC after the rhFGF-2 treatment was further investigated by Western blot analysis. The extracellular signal-regulated kinase (ERK) and c-Jun-N-terminal-kinase (JNK) play an important role in angiogenesis process for tumor growth and metastasis. rhFGF-2 induced activation of ERK after the phosphorylation in FGF receptors. The ERK activation was inhibited completely by NP603 and to a lesser extent by SU16g and SU6668 (Fig. 5). These results indicate that NP603 has potent inhibitory activity on the FGF-2-induced tyrosine phosphorylation of FGF receptor, which resulted in the inhibition of ERK and JNK activation and cellular proliferation in HUVEC.

To evaluate the effect of NP603 on angiogenesis, the HUVEC tube formation assay was performed in which the lengths of the capillary-like tubes formed were measured. NP603 suppressed HUVEC tube formation in a dose dependent manner, in the presence of NP603 HUVECs formed incomplete and narrow tube-like structures (Fig. 6). In contrast, following stimulation with FGF-2, formation of elongated and robust tube-like structures was observed which were organized by a greater number of cells as compared to the control. Treatment with 1, 3, 10, and 25 μM NP603 resulted in

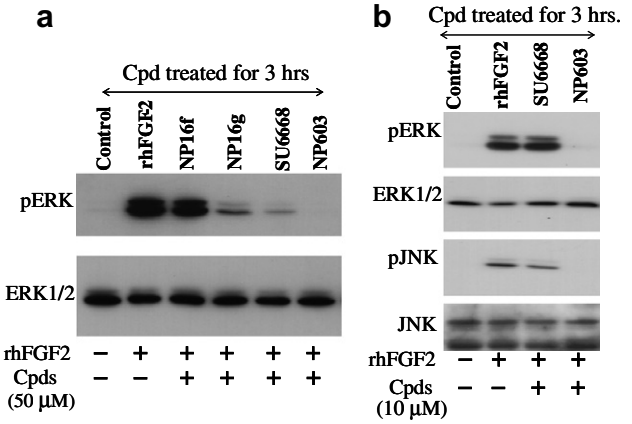

Figure 5. Effect on the intracellular signaling in HUVEC after the rhFGF-2 stimulation, Western blot of total proteins in HUVEC cell lysates with antibodies against ERK1/2, JNK, and phospho-specific ERK1/2 and JNK.

the inhibition of tube formation as compared with the control group. NP603 significantly inhibited tube formation in a concentration-dependent manner. However, when compared with SU6668, NP 603 inhibited tube formation better than SU6668 but not significantly different.

The activity observed lends strong support to the role of Lys514 movement in ligand–receptor binding in order to accommodate the presence of the 3,5-dimethoxyphenyl substituent at the C-6 position in NP603 to locate in the receptor pocket. This leads to an enhancement of the binding capacity. In this regard, the 3,5-dimethoxyphenyl moiety at the C-6 position of indolinone increased the inhibitory potency against FGFR1 as predicted by the modeling study. In order to support this notion, the analogs of mimicking substitution at the C-6 position of the indolin-2-one core (L1–L5) were docked with FGFR1, they all gave better docking energy than SU6668 as expected (Table 2). The binding orientations of L1–L8 docked with FGFR1 are as same as NP603 (Fig. 7). The docking energies of L4 and L8 with 3,5-di-substitution of cyano and with hydroxy-

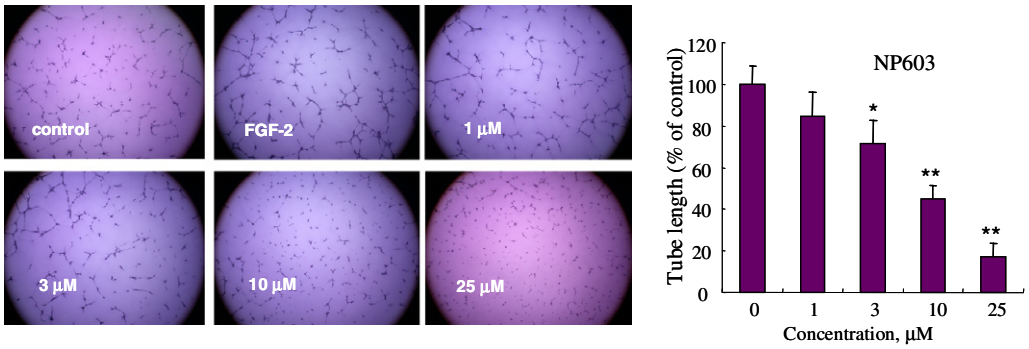

Figure 6. Effect of NP603 on the tube-like formations of HUVEC. HUVEC were seeded onto 96-well plates, which had been coated with 40 μl of Matrigel per well, in the presence of NP603. After a 5-h incubation period at 37 °C, the culture was fixed by glutaraldehyde, and the length of the tube-like formations was evaluated. Original magnification: 5×. A representative experiment is shown, with means ± SD of four wells. $^{*}P < 0.05$, $^{**}P < 0.01$.

Table 2. Docking results of the analogs of mimicking substitution at the C-6 position of the indolin-2-one core

	R	Binding energy (kcal/mol)	Docking energy (kcal/mol)
SU6668	H	−8.49	−10.2
NP603	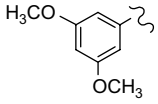	−11.5	−13.3
L1		−11.5	−13.5
L2		−11.4	−13.3
L3	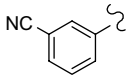	−12.4	−14.4
L4	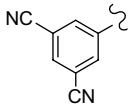	−12.8	−15.4
L5	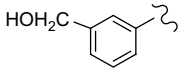	−11.9	−13.9
L6	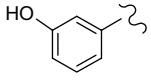	−12.2	−14.2
L7	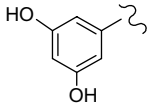	−12.9	−14.7
L8	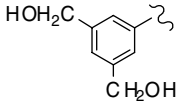	−13.0	−15.6

methyl on phenyl at the C-6 position were lower than NP603, −15.4 kJ/mol for L4 and −15.6 kJ/mol for L8.

The increased interaction of L4 was not only due to the ability to locate in the pocket but also due to the resonance effect from the extended delocalization of π-electrons across two cyano groups. For L8, in addition to fitting in the pocket, the inductive effect of the hydroxymethyl groups substituted on benzene is the additional factor resulting in the enhanced binding leading to the lowest docking energy. Thus, L4 and L5 were chosen for further synthesis and activity testing. The result in Table 2 demonstrated the role of Lys514 movement in ligand–receptor binding to accommodate the hydrophobic interaction at the receptor pocket leading to the enhancement of binding capacity.

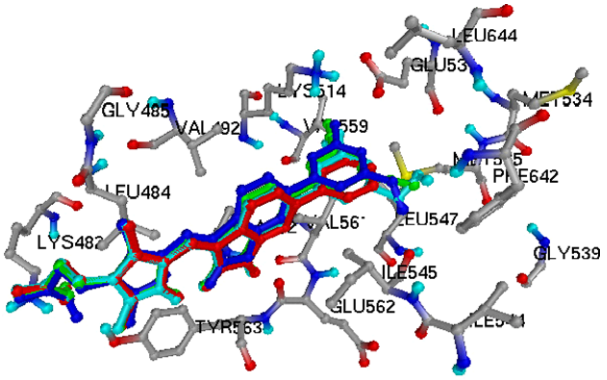

Figure 7. The superposition of docked conformations of L1 (red), L4 (green), L8 (turquoise), and N603 (blue) bound with FGFR1.

Acknowledgments

This work was funded by the Royal Golden Jubilee Project, Thailand Research Fund, and the 21st Century COE project from the Ministry of Education, Culture, Sports, Science and Technology, Japan.

References and notes

1. Plowman, G. D.; Ullrich, A.; Shawver, L. K. *Drug News Perspect.* **1994**, *7*, 334.
2. Straw, L. M.; Shawver, L. K. *Expert Opin. Invest. Drugs* **1998**, *7*, 553.
3. Ullrich, A.; Schlessinger, J. *Cell* **1990**, *61*, 203.
4. Halaban, R. *Can. Met. Rev.* **1991**, *10*, 129.

5. Bishop, J. M. *Science* **1987**, *335*, 305.
6. De Vries, C.; Escobedo, J. A.; Ueno, H.; Houck, K.; Ferrara, N.; Williams, L. T. *Science* **1992**, *255*, 989.
7. Terman, B. I.; Doughervermazen, M.; Carrion, M. E.; Dimitrov, D.; Armellino, D. C.; Gospodarowicz, D.; Bohlen, P. *Biochem. Biophys. Res. Commun.* **1992**, *187*, 1579.
8. Sun, L.; Tran, N.; Tang, F.; App, H.; Hirth, P.; McMahon, G.; Tang, C. *J. Med. Chem.* **1998**, *41*, 2588.
9. Sun, L.; Tran, N.; Liang, C. X.; Tang, F.; Rice, A.; Schreck, R.; Waltz, K.; Shawver, L. K.; McMahon, G.; Tang, C. *J. Med. Chem.* **1999**, *42*, 5120.
10. Mohammadi, M.; Froum, S.; Hamby, J. M.; Schroeder, M. C.; Panek, R. L.; Lu, G. H.; Eliseenkova, A. V.; Green, D.; Schlessinger, J.; Hubbard, S. R. *EMBO J.* **1998**, *17*, 5896.
11. Morris, G. M.; Goodsell, D. S.; Halliday, S.; Huey, R.; Hart, W. E.; Belew, R. K.; Olson, A. J. *J. Comput. Chem.* **1998**, *19*, 1639.
12. Melting point, IR, ^{1}H and ^{13}C NMR, mass, and elemental analysis (C, H, and N) determination. For compound NP603, 3-{5-[6-(3,5-dimethoxy-phenyl)-2-oxo-1,2-dihydro-indol-3-ylidenemethyl]-2,4-dimethyl-1*H*-pyrrol-3-yl}-propionic acid as a mustard red solid: mp 252–254 °C; FTIR (KBr) (cm^{-1}): 3267 (N–H st.), 3087 (aromatic C–H st.), 2945 (aliphatic C–H st.), 1750, 1648 (C=O st.), 1569 (C=C st.), 1447 (bending C–H), 1149 (C–O st.); ^{1}H NMR (300 MHz, DMSO-d_6) δ 13.40 (s, 1H, NH), 10.81 (s, 1H, NH), 7.76 (d, 1H, H7), 7.58 (s, 1H, CH), 7.27 (d, 1H, H5), 7.09 (d, 1H, H4), 6.74 (s, 2H, H2″, H6″), 6.48 (s, 1H, H4″), 3.80 (s, 6H, OMe), 3.35 (s, 3H, OMe), 2.64 (t, 2H, CH_2), 2.38 (t, 2H, CH_2), 2.30 (s, 3H, CH_3), 2.27 (s, 3H, CH_3); ^{13}C NMR (MHz, DMSO-d_6): 174.32, 169.92, 161.15, 143.29, 138.81, 137.90, 134.64, 130.31, 126.31, 126.12, 123.76, 12.46, 120.05, 118.64, 112.35, 107.83, 104.97, 99.38, 55.59, 34.92, 19.83, 12.25, 9.82; MS *m*/*z* 445 [M−H], 446 [M]; elemental analysis CHN (70.12, 5.82, 6.28).
13. Mohammadi, M.; McMahon, G.; Sun, L.; Tang, C.; Hirth, P.; Yeh, B. K.; Hubbard, S. R.; Schlessinger, J. *Science* **1997**, *276*, 955.